Accepted Manuscript
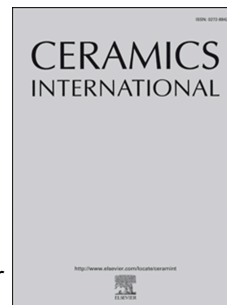
Crystal structure and magnetic properties of LaFe$_{1-x}$Ni$_x$O$_3$ nanomaterials prepared via a simple co-precipitation method

Tien A. Nguyen, Vinh N.T. Pham, Hanh T. Le, Diem H. Chau, V.O. Mittova, Linh T. Tr Nguyen, D.A. Dinh, T.V. Nhan Hao, I. Ya Mittova

Please cite this article as: T.A. Nguyen, V.N.T. Pham, H.T. Le, D.H. Chau, V.O. Mittova, L.T. Tr Nguyen, D.A. Dinh, T.V. Nhan Hao, I. Ya Mittova, Crystal structure and magnetic properties of LaFe$_{1-x}$Ni$_x$O$_3$ nanomaterials prepared via a simple co-precipitation method, *Ceramics International* (2019), doi: https://doi.org/10.1016/j.ceramint.2019.07.178.

CRYSTAL STRUCTURE AND MAGNETIC PROPERTIES OF LaFe$_{1-x}$Ni$_x$O$_3$ NANOMATERIALS PREPARED VIA A SIMPLE CO-PRECIPITATION METHOD

Tien A. Nguyen[1,2+], Vinh N. T. Pham[3,4*], Hanh T. Le[4], Diem H. Chau[4], V. O. Mittova[5],
Linh T. Tr. Nguyen[4+], D. A. Dinh[6+], T. V. Nhan Hao[7+], I. Ya. Mittova[8]

[1]*Department for Management of Science and Technology Development, Ton Duc Thang University, Ho Chi Minh City, Vietnam*
[2]*Faculty of Applied Sciences, Ton Duc Thang University, Ho Chi Minh City, Vietnam*
[3]*Institute of Research and Development, Duy Tan University, Da Nang 550000, Vietnam*
[4]*Ho Chi Minh City University of Education, Ho Chi Minh City 748342, Vietnam*
[5]*Burdenko Voronezh State Medical University, Voronezh 394036 Russia*
[6]*NTT Hi-Tech Institute, Nguyen Tat Thanh University, Ho Chi Minh City 700000, Vietnam*
[7]*Faculty of Physics, University of Education, Hue University, 34 Le Loi Street, Hue City, Vietnam*
[8]*Voronezh State University, Universitetskaya pl. 1, Voronezh 394018 Russia*

* Corresponding author: vinhpnt@hcmue.edu.vn
+ Email addresses: nguyenanhtien@tdtu.edu.vn (Tien A. Nguyen), linhntt@hcmue.edu.vn (Linh T.Tr. Nguyen), ddanh@ntt.edu.vn (D. A. Dinh), tvnhao@hueuni.edu.vn (T. V. Nhan Hao)

Abstract

In this paper, nanostructured Ni-doped LaFeO$_3$ materials were prepared via a simple co-precipitation method involving the hydrolysis of La(III), Fe(III), and Ni(II) cations in hot water with 5% KOH as a precipitating agent. To evaluate the effects of Ni substitution in these products, their structural phases, lattice parameters, crystallite and grain sizes, and magnetic properties were determined. As the Ni content in the LaFe$_{1-x}$Ni$_x$O$_3$ ($x = 0–0.25$) materials increased, the average crystallite size and lattice parameters decreased. Moreover, across the range of Ni-substitution ratios, all magnetic properties correspondingly changed: the coercive force (H_c) value rose from 42.53 to 173.98 Oe. In contrast, the remanent magnetization (M_r) and saturation magnetization (M_s) values decreased from $1.0 \cdot \times 10^{-2}$ to $3.8 \cdot \times 10^{-4}$ emu·g^{-1}, and from $0.24 \cdot \times 10^{0}$ to $0.74 \cdot \times 10^{-4}$ emu·g^{-1}, respectively. These predictable changes provide a sound foundation for the fabrication and application of magnetic materials based on nanostructured Ni-doped LaFeO$_3$ substrates.

Keywords: Nanocrystal, Ni-doped LaFeO$_3$, crystal structure, magnetic properties, co-precipitation method.

1. Introduction

LaFeO$_3$, a perovskite-type material (general formula of ABO$_3$, where A and B are a rare earth element and 3d transition metal, respectively) with an orthorhombic structure, has attracted great interest due to its promise for use in advanced technologies such as solid oxide fuel cells [1], catalysts [2], chemical sensors [3], magnetic materials [4], and oxygen permeation membranes [5].

For example, a Ni-doped $LaFeO_3$ perovskite was used [6] to fabricate the cathode material for a solid oxide fuel cell, and displayed (1) good catalytic activity for oxygen reduction at an operating temperature ≥ 700 °C and (2) thermal expansion properties matched to those of the electrolyte and interconnect. To successfully develop nanostructured Ni-doped $LaFeO_3$ perovskites, it is essential to thoroughly understand the magnetic properties of $LaFeO_3$ and $LaNiO_3$, as well as the spin states of Fe^{3+} and Ni^{3+} ions. $LaFeO_3$ is known as an anti-ferromagnetic insulator at a Néel temperature of 740 K, while $LaNiO_3$ is a paramagnetic metallic oxide down to lowest temperatures [10]. Fe^{3+} is in the high spin state (t_{2g}^3, e_g^2), while Ni^{3+} is in the low spin state (t_{2g}^6, e_g^1). The metal-to-insulator transition has been attributed to the disorder induced by the difference in the $3d$ energy levels of Fe and Ni in Ni-doped $LaFeO_3$ materials [7]. Ni-doped $LaFeO_3$ materials have also been investigated for many purposes, including catalysis [8, 9], electrical conductivity [10], and oxygen permeability [11].

Generally, to synthesise nanostructured Ni-doped $LaFeO_3$ materials, methods similar to those used in the preparation of $LaFeO_3$ compounds have been applied, including solid-state [12], electrochemical [13], and sol-gel combustion [14] techniques. The solid-state reaction requires high temperature, while the sol-gel method involves a time-consuming sol-gelation process and precise control to form single-phase crystals. Moreover, the use of organic agents in sol-gel fabrication may introduce undesirable impurities which can directly affect the magnetic and electronic properties of the products [14, 15]. Thus, although each approach possesses both advantages and disadvantages, the optimal selection of a method to produce the desired magnetic and electronic properties remains challenging.

In this work, nanostructured Ni-doped $LaFeO_3$ materials were prepared via a simple co-precipitation method through the hydrolysis of cations in hot water ($t > 90$ °C), without the addition of organic agents. The efficiency of this approach was validated by measuring the structural and magnetic properties of the synthesized products by appropriate characterization techniques.

2. Experimental

To synthesise the $LaFe_{1-x}Ni_xO_3$ perovskites ($x = 0$, 0.1, 0.15, 0.2, and 0.25), analytical grade $La(NO_3)_3 \cdot 6H_2O$, $Fe(NO_3)_3 \cdot 9H_2O$, $Ni(NO_3)_2 \cdot 6H_2O$, and KOH (Merck, Germany) were used as starting materials. The synthesis process was similar to that described in our previous work [16]. A solution containing an appropriate ratio of La^{3+}, Fe^{3+}, and Ni^{2+} ions was gradually added to hot water (> 90 °C) and stirred continuously. The mixture was cooled to room temperature (25–30 °C) and 5% KOH solutions was slowly added until pH 7 was attained. The precipitates were continuously stirred for 30 min, filtered, washed carefully with deionised water, and dried in air.

The crystallisation process was monitored via thermogravimetric analysis (TGA) on a LABSYS evo 1600°C instrument (SETARAM Instrumentation, France), by heating the sample in an aluminium oxide crucible under nitrogen at a rate of 10 °C min^{-1}.

The structure and phase composition of the materials were investigated by X-ray diffraction (XRD, D8-ADVANCE, Bruker, Inc., Germany) with Cu K$_\alpha$ radiation (λ = 1.540 Å) using a step size of 0.02° in range of 20 to 80°. The crystallite sizes of LaFe$_{1-x}$Ni$_x$O$_3$ (D_{XRD}, nm) were determined based on Scherrer's equation:

$$D = \frac{0.89\lambda}{\beta\cos\theta},\qquad(1)$$

where β is the full-width at half maximum (FWHM), and θ is the diffraction angle of the maximum reflection.

Lattice constants (a, b, c) and unit cell volumes (V) were calculated using the formulae presented in Ref. [17]:

$$\frac{1}{d^2} = \frac{h^2}{a^2} + \frac{k^2}{b^2} + \frac{l^2}{c^2},\qquad(2)$$

$$V = a \cdot b \cdot c.\qquad(3)$$

The morphologies of the nanostructured LaFe$_{1-x}$Ni$_x$O$_3$ materials were determined by scanning electron microscopy (FE-SEM, Hitachi S-4800, Japan) and transmission electron microscopy (TEM, JEOL-1400, Japan).

The magnetic properties of the samples, including the coercive force H_c, remanent magnetization M_r, saturation magnetization M_s, and maximum energy product $(BH)_{max}$ were investigated at 300 K via a vibrating sample magnetometer (VSM, Microsense EV11, Japan).

3. Results and discussion

Structure and morphology of LaFeO$_3$

A sample of undoped LaFeO$_3$ was prepared by the general method and subjected to TGA, with the results shown in Fig. 1. The onset of initial weight loss (~23.33 %) starts slowly near 75 °C, reaches a maximum at ~125 °C, and finishes at ~340 °C. Below 340 °C, the weight loss is due to the removal of the water of crystallisation and dehydration of Fe$_2$O$_3 \cdot y$H$_2$O (y = 1÷5) [18]. The weight loss between 300–550 °C (~11.71 %) may stem from the pyrolysis of LaO(OH)$\cdot m$H$_2$O [19]. Further heating causes a small weight loss (~6.83%) at ~780 °C that is attributed to the release of CO$_2$ from La$_2$O(CO$_3$)$_2 \cdot$1.4H$_2$O or La$_2$(CO$_3$)$_3 \cdot$8H$_2$O [20–22]. The release of CO$_2$ ends at ~850 °C, which is higher than that of H$_2$O (~550 °C) because the La–CO$_3$ bond is stronger than that of La–

OH [22–24]. No further weight loss occurs thereafter, indicating that there is no change in the phase of the product formed at temperatures higher than the considered range.

Figure 2 shows the XRD pattern of the undoped LaFeO$_3$ product after annealing at 850 °C, corresponding to the decomposition temperature selected on the basis of the TGA results. The diffraction pattern reveals only the presence of the orthorhombic LaFeO$_3$ phase (JCPDS file No. 37-1493). The average crystallite size of the LaFeO$_3$ product, according to Eq. (1), is ~28.72 nm, while the lattice parameters and unit cell volume calculated according to Eqs. (2) and (3) are: a = 5.573 Å, b = 7.849 Å, c = 5.558 Å, and V = 243.121 Å^3 (Table 1). This confirms that the crystallisation temperature of the LaFeO$_3$ perovskite phase is near 850 °C, as anticipated by the corresponding thermal decomposition curve (Fig. 1).

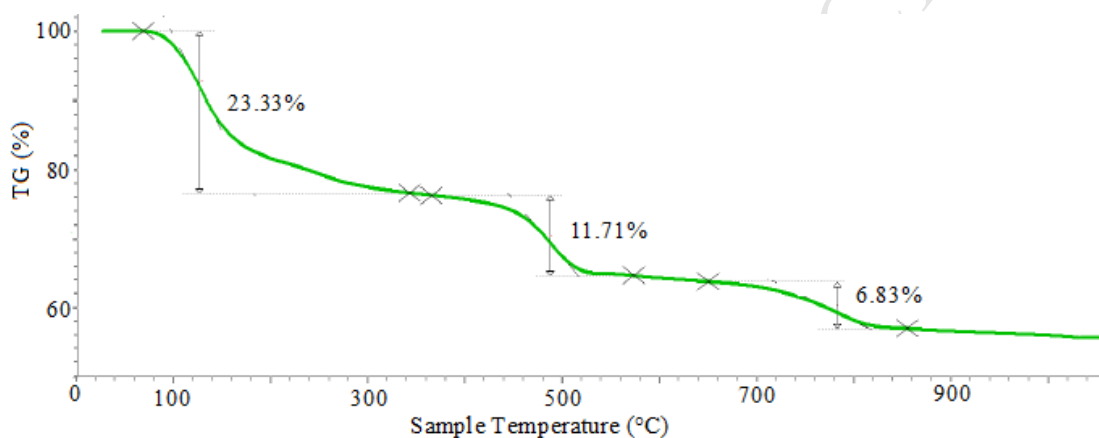**Fig. 1.** TGA curve of the undoped LaFeO$_3$ product.

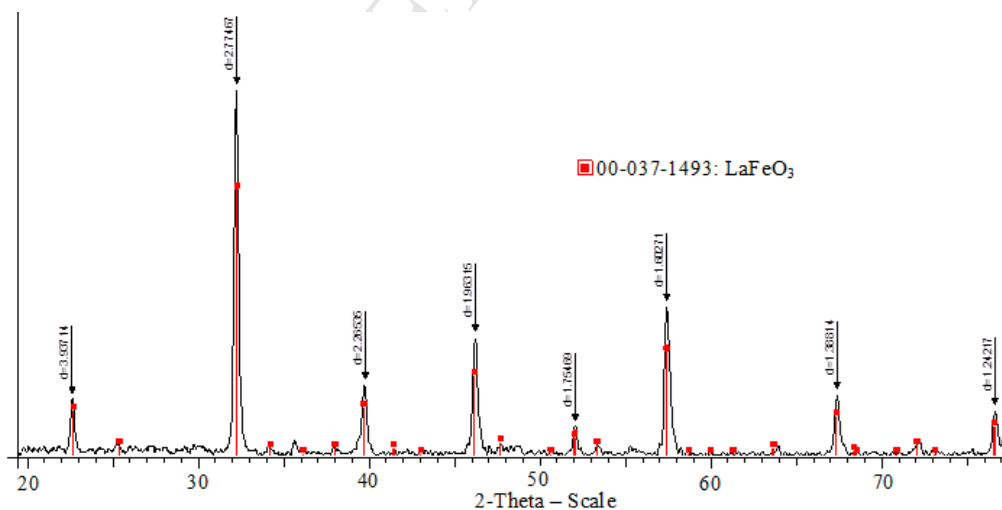**Fig. 2.** XRD pattern of LaFeO$_3$ annealed at 850 °C for 1 h.

The SEM and TEM images (Fig. 3) of the sample show that the LaFeO$_3$ perovskite particles have an average size of ~30–50 nm.
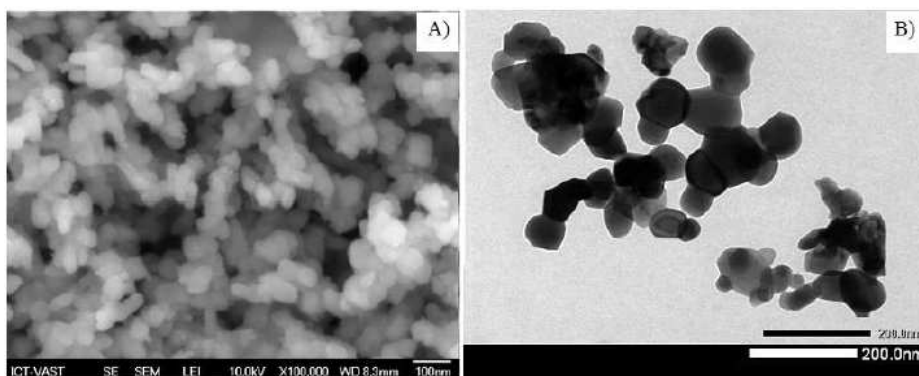
4

Fig. 3. SEM (A) and TEM (B) images of LaFeO$_3$ nanomaterial annealed at 850 °C for 1 h.

Structures and morphologies of nanostructured LaFe$_{1-x}$Ni$_x$O$_3$ (x = 0.1, 0.15, 0.2, and 0.25)

Based on the TGA and XRD results for the undoped LaFeO$_3$ sample, a temperature of 850 °C was chosen for the fabrication of the LaFe$_{1-x}$Ni$_x$O$_3$ (x = 0.1, 0.15, 0.2, and 0.25) perovskite materials. Figure 4 shows the XRD pattern of the LaFe$_{0.8}$Ni$_{0.2}$O$_3$ product compared with those of the NiO and Fe$_2$O$_3$ components, which were independently prepared under similar conditions. The LaFe$_{0.8}$Ni$_{0.2}$O$_3$ product has the specific peaks of the LaFeO$_3$ orthorhombic phase (JCPDS file No. 37-1493) with no detectable secondary phase. The XRD patterns in Fig. 5 reveal no significant differences between the samples having different Ni-doping ratios.

All the XRD patterns of LaFe$_{1-x}$Ni$_x$O$_3$ (x = 0.1, 0.15, 0.2, and 0.25) (Fig. 5) show the existence of a single-phase orthorhombic perovskite (*Pnma* space group, No. 62). We can therefore conclude that the simple co-precipitation method is appropriate for the fabrication of LaFe$_{1-x}$Ni$_x$O$_3$ materials with $x \leq 0.25$.
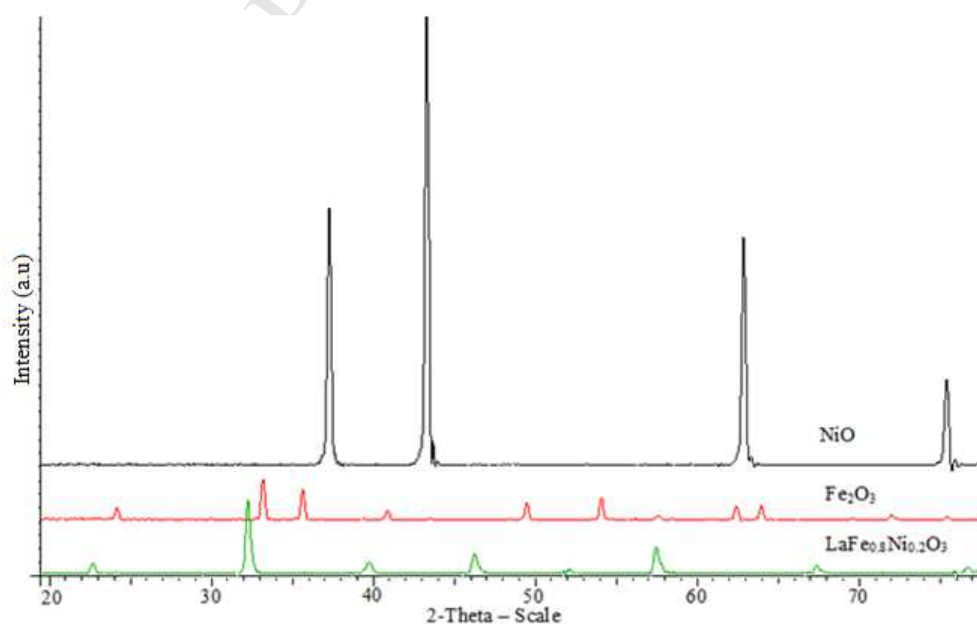

Fig. 4. XRD patterns of LaFe$_{0.8}$Ni$_{0.2}$O$_3$, NiO, and Fe$_2$O$_3$ annealed at 850 °C for 1 h.

5

Remarkably, the XRD peaks tend to broaden and shift toward a higher 2θ position (right-shift) due to the substitution of Ni in the $LaFeO_3$ lattice. Similar phenomena have also been observed in other studies [25–27]. The shift of peaks toward higher 2θ values indicates a reduction of the *a, b, c,* and *V* values of the $LaFe_{1-x}Ni_xO_3$ samples relative to the pure $LaFeO_3$ sample (Table 1). These reductions in the unit cell size may originate for several reasons: (1) Ni(III) ions are substituted into the perfect crystalline $LaFeO_3$ with fine crystallite size of the crystalline $LaFeO_3$ facilitates Ni(III) ion substitution (Fig. 2); (2) the diameter of the substituted Ni(III) ion is smaller than that of the Fe(III) ion [19]; and (3) the sequential increase of substituted-Ni content leads to lattice defects that raise the internal stress and restrain the growth of the crystals. Consequently, the presence of Ni in the $LaFeO_3$ lattice broadens the XRD peaks of the $LaFe_{1-x}Ni_xO_3$ samples and reduces the crystallite size from 28.72 to 23.59 nm (Table 1).
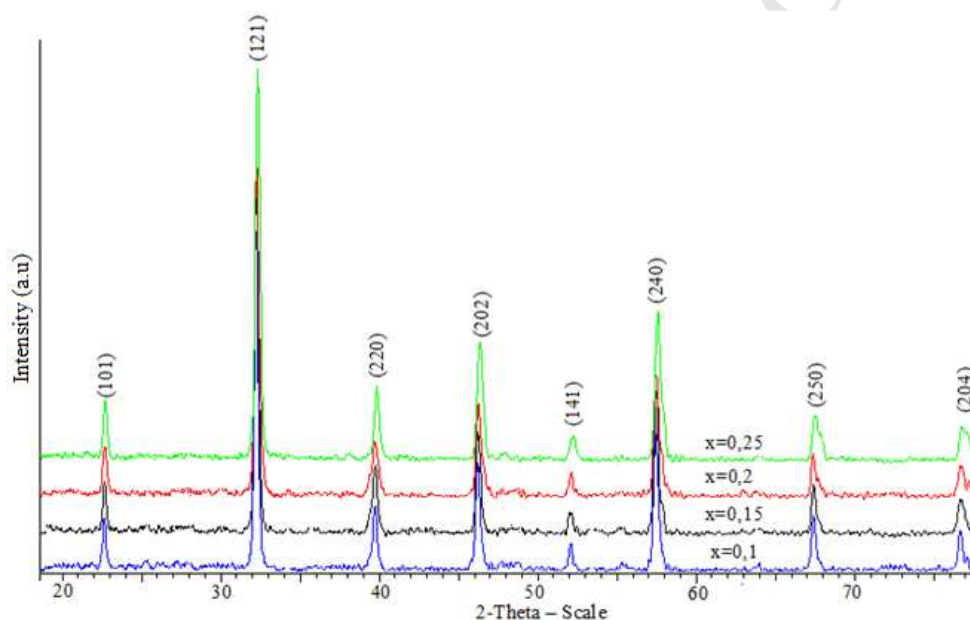

Fig. 5. XRD patterns of $LaFe_{1-x}Ni_xO_3$ (x = 0.1, 0.15, 0.2, and 0.25) samples calcined at 850 °C for 1 h.

Table 1. Lattice parameters and crystallite sizes of $LaFe_{1-x}Ni_xO_3$ samples annealed at 850 °C for 1 h.

$LaFe_{1-x}Ni_xO_3$	$2\theta_{(121)}$, °	D, nm	Lattice constants, Å			V, Å^3
			a	b	c	
$x = 0$	32.1900	28.72	5.573	7.849	5.558	243.121
$x = 0.1$	32.1886	26.02	5.544	7.866	5.560	242.467
$x = 0.15$	32.1979	27.51	5.544	7.845	5.584	242.863
$x = 0.2$	32.2107	28.99	5.531	7.879	5.564	242.472
$x = 0.25$	32.3066	23.59	5.546	7.830	5.531	240.185

TEM images of the $LaFe_{0.8}Ni_{0.2}O_3$ and $LaFe_{0.75}Ni_{0.25}O_3$ samples (Fig. 6), however, do not show significant changes in particle size or shape as the concentration of Ni changes. The Ni-doped

6

LaFeO$_3$ particles are relatively uniform in shape (spherical) and size (30–50 nm), as in the case of the undoped LaFeO$_3$.
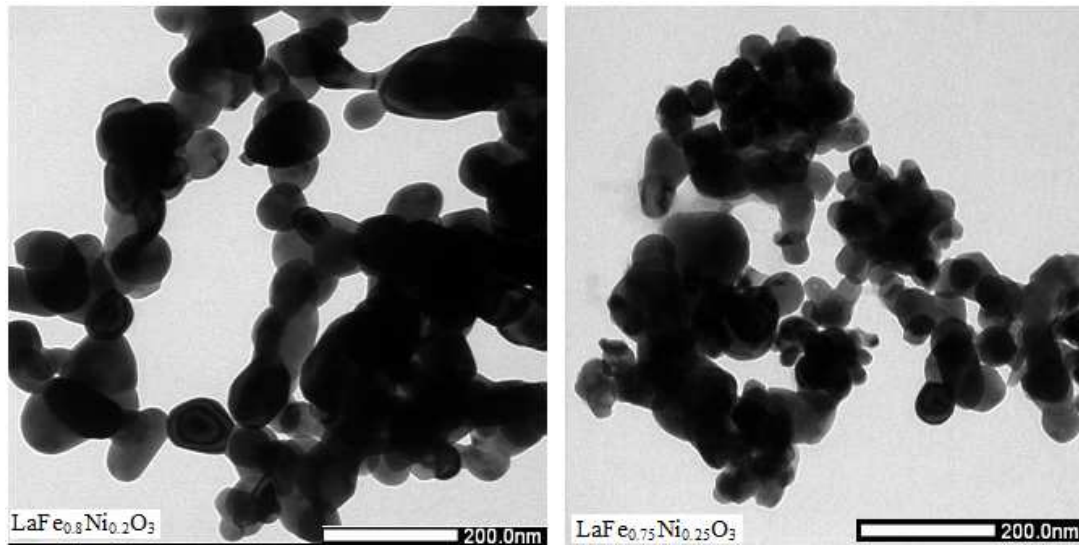

Fig. 6. TEM images of nanostructured LaFe$_{0.8}$Ni$_{0.2}$O$_3$ and LaFe$_{0.75}$Ni$_{0.25}$O$_3$ materials annealed at 850 °C for 1 h.

Magnetic properties of nanostructured LaFe$_{1-x}$Ni$_x$O$_3$ (x = 0, 0.1, 0.15, 0.2, and 0.25)

Magnetic measurements at room temperature for the LaFe$_{1-x}$Ni$_x$O$_3$ ($x = 0$, 0.1, 0.15, 0.2, and 0.25) samples indicate that the substitution of Ni in the LaFeO$_3$ crystal lattice affects not only the structural characteristics but also the magnetic properties of the products (Table 2 and Fig. 7). While the LaFeO$_3$ nanomaterial, with a coercive force H_c of 42.53 Oe, can be considered a soft magnetic material, the LaFe$_{1-x}$Ni$_x$O$_3$ products become hard magnetic materials with higher H_c (> 150 Oe). The substitution of Ni into the LaFeO$_3$ lattice causes an increase in the magneto-crystalline anisotropy, and therefore, H_c for the LaFe$_{1-x}$Ni$_x$O$_3$ materials increases. For LaFe$_{1-x}$Ni$_x$O$_3$ with $x =$ 0.1–0.25, H_c increases as x in range of 0.1 to 0.2, whereas, at $x = 0.25$, H_c declines. This can be explained by the effect of the crystallite size on H_c. Nanoscale particles ($D < 100$ nm) can be considered as single-domain particles. Then, H_c depends on the particle size according to the following formula [28]:

$$H_c = g - \frac{h}{D^{3/2}},\tag{4}$$

where g and h are constants, and D is the particle diameter. Clearly, H_c will increase with the particle size. Indeed, when x is increased from 0.1 to 0.2, the crystallite size rises from 26.02 to 28.99 nm and H_c also increases from 168.14 to 173.98 Oe. However, for the LaFe$_{0.75}$Ni$_{0.25}$O$_3$ sample, the crystallite size is reduced to 23.59 nm, and H_c drops to 160.76 Oe.

7

Substitution by Ni reduces the remanent magnetization M_r and saturation magnetization M_s of the samples (Table 2). The decline of M_s at higher values of x is also related to the decrease in the crystallite size. The smaller the particle, the larger its surface area-to-volume ratio. This leads to the existence of non-magnetized surface areas and reduces the M_s value. Similar phenomena were also reported for several other series (($La_{1-x}Sr_x$)($Fe_{1-x}Ni_x$)O_3 [29], $PrFe_{1-x}Ni_xO_3$, and $GdFe_{1-x}Ni_xO_3$ [27, 30]). Therefore, changes in the doping elements and their concentrations can alter the magnetic properties of perovskite-type nanomaterials, a phenomenon which may be applied in tuning the properties of magnetic materials for various applications.

Table 1. Magnetic properties of $LaFe_{1-x}Ni_xO_3$ nanomaterials calcined at 850 °C for 1 h.

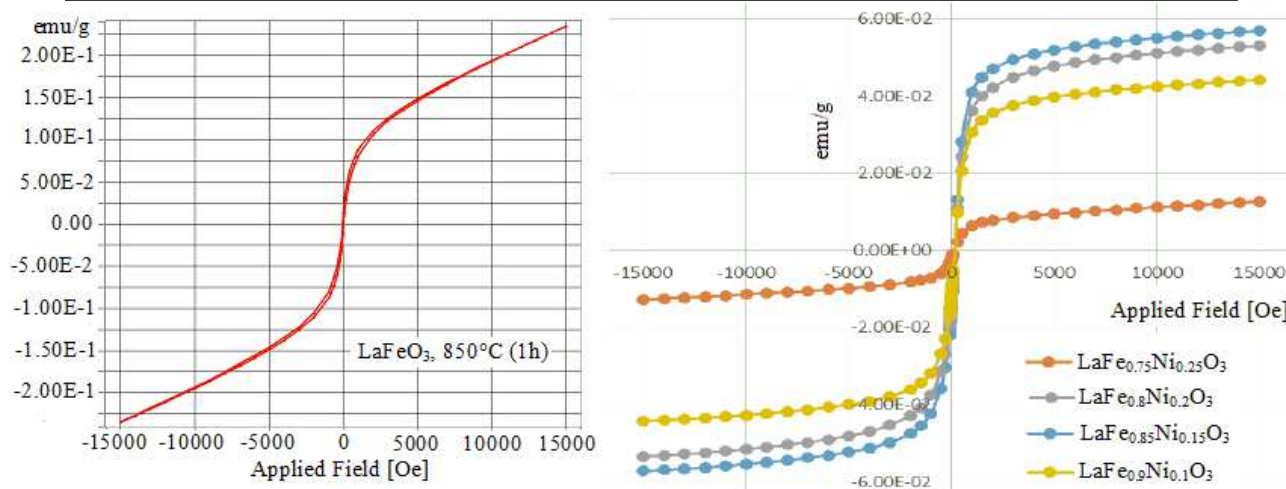| Sample	H_c, Oe	M_r, emu·g^{-1}	M_s, emu·g^{-1}
$LaFeO_3$	42.53	$1.0 \cdot \times 10^{-2}$	$0.24 \cdot \times 10^0$
$LaFe_{0.9}Ni_{0.1}O_3$	168.14	$4.0 \cdot \times 10^{-4}$	$15.7 \cdot \times 10^{-4}$
$LaFe_{0.85}Ni_{0.15}O_3$	168.87	$5.7 \cdot \times 10^{-4}$	$21.1 \cdot \times 10^{-4}$
$LaFe_{0.8}Ni_{0.2}O_3$	173.98	$5.2 \cdot \times 10^{-4}$	$20.2 \cdot \times 10^{-4}$
$LaFe_{0.75}Ni_{0.25}O_3$	160.76	$3.8 \cdot \times 10^{-4}$	$0.74 \cdot \times 10^{-4}$

Fig. 7. Field dependence of the magnetization of the $LaFe_{1-x}Ni_xO_3$ nanomaterials annealed at 850 °C for 1 h.

4. Conclusions

$LaFe_{1-x}Ni_xO_3$ (x = 0, 0.1, 0.15, 0.2, and 0.25) perovskite-type materials were successfully prepared via a simple co-precipitation method without the use of organic agents. Single-phase $LaFe_{1-x}Ni_xO_3$ products formed after annealing at 850 °C for 1 h had grain sizes in the range of 30 to 50 nm and unit cell volumes in the range of 240 to 243 Å^3. As the Ni content in the $LaFe_{1-x}Ni_xO_3$ products increased from 0 to 0.25, the H_c value increased, whereas the M_r and M_s values decreased. These predictable changes serve as a good foundation for the fabrication and application of

magnetic materials based on nanostructured Ni-doped $LaFeO_3$ substrates. As a result, the original $LaFeO_3$ nanomaterial, which had a low H_c (42.53 Oe), small M_r (0.01 emu·g^{-1}), and high M_s (0.24 emu·g^{-1}), is suitable for instruments operating at high magnetic field. In contrast, the Ni-doped $LaFeO_3$ materials, with high H_c ($\gg$100 Oe) and low M_s ($0.74 \times 10^{-4} - 21.1 \times 10^{-4}$ emu·g^{-1}), can be used to produce permanent magnets and magnetic tapes.

Conflict of interest

The authors maintain that they have no conflict of interest with respect to this communication.

Notes and references

1. M. H. Hung, M. V. M. Rao, and D-Sh. Tsai, Microstructure and electrical properties of calcium substituted $LaFeO_3$ as SOFC cathode, *Materials Chemistry and Physics*, 2007, **101(2-3)**, 297-302.
2. Y-G. Cho, K-H. Choi, Y-R. Kim, J-S. Jung, and S-H. Lee, Characterization and catalytic properties of surface La-rich $LaFeO_3$ perovskite, *Bulletin of the Korean Chemical Society*, 2009, **30(6)**, 1368-1370.
3. V. Lantto, S. Saukko, N. N. Toan, L. F. Reyes, and C. G. Granqvist, Gas sensing with perovskite-like oxides having ABO_3 and BO_3 structures, *Journal of Electroceramics*, 2004, **13(1-3)**, 721-726.
4. Y. Li, H. Zhang, X. Liu, Q. Chen, and Q. Chen, Electrical and magnetic properties of $La_{1-x}Sr_xMnO$ ($0.1 \leq x \leq 0.25$) ceramics prepared by sol-gel technique, *Ceramics International*, 2019, **45(13)**, 16323-16330.
5. A. L. Shaula, V. V. Kharton, N. P. Vyshatko, E. V. Tsipis, M. V. Patrakeev, F. M. B. Marques, and J. R. Frade, Oxygen ionic transport in $SrFe_{1-y}Al_yO_{3-\delta}$ and $Sr_{1-x}Ca_xFe_{0.5}Al_{0.5}O_{3-\delta}$, *Journal of the European Ceramic Society*, 2005, **25**, 489-499.
6. K. Huang, H. Y. Lee, and J. B. Goodenough, Sr- and Ni-doped $LaCoO_3$ and $LaFeO_3$ perovskites: New cathode materials for solid-oxide fuel cells, *Journal of the Electrochemical Society*, 1998, **145(9)**, 3220-3227.
7. A. Chainani, D. D. Sarma, I. Das, and E. V. Sampathkumaran, Low-temperature electrical conductivity of $LaNi_{1-x}Fe_xO_3$, *Journal of Physics: Condensed Matter*, 1996, **8**, L631-L636.
8. X. Li, H. Shi, W. Zhu, S. Zuo, X. Lu, S. Luo, and Y. Chen, Nanocomposite $LaFe_{1-x}Ni_xO_3$/Palygorskite catalyst for photo-assisted reduction of NO_x: Effect of Ni doping, *Applied Catalysis B: Environmental*, 2018, **231**, 92-100.
9. U. Oemar, P. Ang, K. Hidajat, and S. Kawi, Promotional effect of Fe on perovskite $LaNi_xFe_{1-x}O_3$ catalyst for hydrogen production via steam reforming of toluene, *International Journal of Hydrogen Energy*, 2013, **38**, 5525-5534.
10. R. Kumar, R. Choudhary, M. Khan, J. Srivastava, C. Bao, H. Tsai, and W. Pong, Structural, electrical transport and x-ray absorption spectroscopy studies of $LaFe_{1-x}Ni_xO_3$ ($x \leq 0.6$), *Journal of Applied Physics*, 2005, **97**, 093526.
11. V. Kharton, A. Viskup, E. Naumovich, and V. Tikhonovich, Oxygen permeability of $LaFe_{1-x}Ni_xO_{3-\delta}$ solid solutions, *Materials Research Bulletin*, 1999, **34(8)**, 1311-1317.
12. M. Idrees, M. Nadeem, M. Mehmood, M. Atif, K. H. Chae, and M. M. Hassan, Impedance spectroscopic investigation of delocalization effects of disorder induced by Ni doping in $LaFeO_3$, *Journal of Physics D: Applied Physics*, 2011, **44(10)**, 105401.
13. X.-D. Zhou, E. Thomsen, Q. Cai, J. Yang, B. Scarfino, W. James, W. Yelon, H. U. Anderson, and L. R. Pederson, Electrical, thermoelectric, and structural properties of $La(Fe,M)O_3$ (M = Mn, Ni, and Cu), *Journal of the Electrical Society*, 2006, **153**, J133-J138.
14. A. Saad, W. Khan, P. Dhiman, A. Naqvi, and M. Singh, Structural, optical and magnetic properties of perovskite $(La_{1-x}Sr_x)(Fe_{1-x}Ni_x)O_3$, ($x = 0.0, 0.1$ & 0.2) nanoparticles, *Electronic Materials Letters*, 2013, **9(1)**, 77-81.
15. A. T. Nguyen, I. Ya. Mittova, M. V. Knurova, V. O. Mittova, T. M. T. Nguyen, and C. N. B. Hoang, Sol-gel preparation and magnetic properties of nanocrystalline lanthanum ferrite, *Russian Journal of General Chemistry*, 2014, **84(7)**, 1261-1264.
16. A. T. Nguyen, H. D. Chau, T. T. L. Nguyen, V. O. Mittova, and I. Ya. Mittova, Structural and magnetic properties of $YFe_{1-x}Co_xO_3$ ($0.1 \leq x \leq 0.5$) perovskite nanomaterials synthesized by co-precipitation method, *Nanosystems: Physics, Chemistry, Mathematics*, 2018, **9(3)**, 424-429.
17. M. Yousefi, S. S. Zeid, and Kh. M. Mozhgan, Synthesis and characterization of nano-structured perovskite type neodymium orthoferrite $NdFeO_3$, *Current Chemistry Letters*, 2017, **6**, 23-30.
18. A. G. Belous, E. V. Pashkova, V. A. Elshanskii, and V. P. Ivanitskii, Effect of precipitation conditions on the phase composition, particle morphology and properties of iron(III, II) hydroxide precipitates, *Inorganic Materials*, 2000, **36(4)**, 343-351.

19. C. E. Housecroft & A.G. Sharpe, *Inorganic Chemistry*, Essex, England: Pearson Education Limited, 2012.

20. N. Imanaka, Physical and chemical properties of rare earth oxides, *Binary Rare Earth Oxides*, Kluwer Academic Publishers, 2004, 111-113.

21. N. Kozo, H. Wakita, and A. Mochizuki, The synthesis of crystalline rare earth carbonates, *Bulletin of the Chemical Society of Japan*, 1973, **46(1)**, 152-156.

22. J. Liu, G. Wang, L. Lu, Y. Guo, and L. Yang, Facile shape-controlled synthesis of lanthanum oxide with different hierarchical micro/nanostructures for antibacterial activity based on phosphate removal, *RSC Advances*, 2017, **7**, 40965-40972.

23. L. N. Komissarova, V. M. Shatskii, G. Ya. Pushkina, L. G. Shcherbakova, L. G. Mamsurova, and E. G. Sukhanova, Soedineniya redkozemel'nykh elementov. Karbonaty, oksalaty, nitraty, titanaty (Compounds of the rare earth elements: Carbonates, oxalates, nitrates, and titanates), Moscow: Nauka, 1984 [in Russian].

24. A. T. Nguyen, I. Ya. Mittova, O. V. Almjasheva, S. A. Kirillova, and V. V Gusarov, Influence of the preparation conditions on the size and morphology of nanocrystalline lanthanum orthoferrite, *Glass Physics and Chemistry*, 2008, **34(6)**, 756-761.

25. C. Feng, S. Ruan, J. Li, B. Zou, J. Luo, W. Chen, and F. Wu, Ethanol sensing properties of $LaFe_{1-x}Co_xO_3$ nanoparticles: Effects of calcination temperature, Co-doping, and carbon nanotube-treatment, *Sensors and Actuators B: Chemical*, 2011, **155(1)**, 232-238.

26. A. T. Nguyen and T. T. L. Nguyen, Structure and magnetization of $LaFe_{1-x}Co_xO_3$ perovskite nanomaterials synthesized by co-precipitation method, *Journal of Science ofHanoi National University of Education*, 2016, **61(9)**, 68-74.

27. F. A. Mir, S. K. Sharma, and R. Kumar, Magnetizations and magneto-transport properties of Ni-doped $PrFeO_3$ thin films, *Chinese Physics B*, 2014, **23(4)**, 048101.

28. B. D. Cullity and C. D. Graham, *Introduction to Magnetic Materials*, Piscataway, NJ: John Wiley & Sons, 2011.

29. M. Rydén, A. Lyngfelt, T. Mattisson, D. Chen, A. Holmen, and E. Bjørgum, Novel oxygen-carrier materials for chemical-looping combustion and chemical-looping reforming; $La_xSr_{1-x}Fe_yCo_{1-y}O_{3-\delta}$ perovskites and mixed-metal oxides of NiO, Fe_2O_3 and Mn_3O_4, *International Journal of Greenhouse Gas Control*, 2008, **2(1)**, 21-36.

30. P. Kaur, K. K. Sharma, R. Pandit, R. Kumar, R. K. Kotnala, J. Shah, Temperature dependent dielectric and magnetic properties of $GdFe_{1-x}Ni_xO_3$ ($0.0 \leq x \leq 0.3$) orthoferrites, *Journal of Applied Physics*, 2014, **115**, 224102-1–224102-7.